



Geophysical Monitoring of Landslides—A Step Closer Towards Predictive Understanding?

Sebastian Uhlemann, Jonathan Chambers, Philip Meldrum, Patrick McClure, and Baptiste Dafflon

Abstract

Landslide early warning is still mostly reliant on precipitation thresholds, which can fail to address the subsurface conditions causing slope instabilities. Here we introduce a novel approach combining the latest developments in geophysical and environmental monitoring, with hydrological and geomechanical modelling to provide robust estimates of current and future Factors-of-Safety of slopes, which we propose may be a robust measure for developing early warning thresholds. We aim to develop a methodology that can predict slope instabilities by estimating the causing subsurface conditions in near-real time, thereby allowing for timely early warning to vulnerable communities and implementation of mitigation measures. It is shown here applied to a hillslope with a history of slope failure, using simplified hydrological and geomechanical models. During the monitoring period, precipitation events are shown to give rise to the local water table, thereby reducing the Factor-of-Safety of the slope. It underlines the value of predicting the effect of future storm (or precipitation) events, that imply an additional reduction and hence an increased risk for slope

failure. Although applied to a local hillslope, the same approach can be upscaled to regional scales using emerging and established remote sensing and wireless sensor networks.

Keywords

Electrical resistivity tomography • Landslide monitoring • Slope stability • Data-driven hydro-geomechanical modelling

Introduction

Landslides are a major and common natural hazard. They endanger communities and critical infrastructure, and have caused more than 28,000 fatalities and more than \$1.8 billion in direct damage within the last decade worldwide. While seismic events are a likely triggering mechanism in many areas, exceptional and prolonged precipitation events triggering landslides are more frequent. This has been shown, e.g., during the 1997–98 El Niño winter storms, which caused more than 300 landslides in the San Francisco Bay Area damaging public and private property, with an estimated direct cost of \$158 million (Godt 1999). Climate change, causing more frequent weather extremes, is likely to increase the occurrence of shallow landslides locally and worldwide. In order to mitigate the risk, there is a need to improve our understanding of shallow, rainfall-induced landslide dynamics, which are mostly controlled by hydrological processes (Bogaard and Greco 2016). These processes are known to be spatially and temporally highly heterogeneous. However, the state-of-the-art is still monitoring surface expressions of slope failure (i.e. active failure), either via remote sensing or direct field observations, rather than monitoring subsurface hydrological properties. Landslide early warning systems are also still mostly reliant on precipitation records, rather than soil moisture

S. Uhlemann (✉)

Lawrence Berkeley National Laboratory, Energy Geosciences Division, One Cyclotron Road, Berkeley, CA 94720, USA
e-mail: suhlemann@lbl.gov

J. Chambers · P. Meldrum

British Geological Survey, Environmental Science Centre, Keyworth, NG12 5GG, UK
e-mail: jecha@bgs.ac.uk

P. Meldrum

e-mail: pime@bgs.ac.uk

P. McClure · B. Dafflon

Lawrence Berkeley National Laboratory, Climate & Ecosystem Science Division, One Cyclotron Road, Berkeley, CA 94720, USA
e-mail: ptm@lbl.gov

B. Dafflon

e-mail: bdafflon@lbl.gov

© Springer Nature Switzerland AG 2021

N. Casagli et al. (eds.), *Understanding and Reducing Landslide Disaster Risk*, ICL Contribution to Landslide Disaster Risk Reduction, https://doi.org/10.1007/978-3-030-60311-3_8

measurements, and hence their reliability has been questioned (Marra 2019).

Recent developments of geophysical techniques, geoelectrical monitoring in particular, and wireless sensor networks enable near real-time monitoring of subsurface hydrological properties and processes at unprecedented spatial and temporal resolution. The novelty of this study lies in the integration of this high-resolution data with hydro-geomechanical models. Eventually, this will bring us one step closer towards predicting and reliable early warning of slope instability.

While conventional hydrological monitoring data can readily be implemented in geomechanical modelling (e.g., Bordoni et al. 2015; Springman et al. 2013), and geophysical and hydrological models can be coupled (Hinnell et al. 2010; Irving and Singha 2010; Singha et al. 2015; Johnson et al. 2017), the link between geophysics and geomechanical modelling has not yet been established. Bridging this gap should improve the assessment of Factors-of-Safety (FoS) of slopes by incorporating spatially and temporarily distributed measurements of soil moisture, and should enable us to forecast slope stability by including weather predictions (i.e. recharge rates) and estimating related subsurface flow conditions. It is anticipated that the real-time FoS and its predicted future change can be used as a reliable early warning threshold, e.g. if the predicted FoS becomes close to 1, a warning should be issued.

Here, we present this approach by linking geophysical and environmental data with simplified slope stability and hydrological flow models. We show that including subsurface data into the FoS calculation improves this estimate and that we can use geophysical data to inform hydrological models to derive subsurface flow related to slope stability. This approach is exemplary shown applied to a site in Northern California, which has a long-standing history of slope instabilities due to prolonged and intense rainfall.

Recent Advances in Subsurface Imaging and Modelling

Recent advances in geophysical data acquisition and processing allow for near-real time monitoring of subsurface moisture dynamics at high spatial (10's of cm's to m's) and temporal (hourly to daily) resolution. By using low-cost, low-powered instrumentation, long-term monitoring at remote locations has become feasible, while data can be analysed at near-real time thanks to wireless data communication technologies (Huntley et al. 2019). This has led to an increased number of geophysical monitoring studies that are recording subsurface dynamics over longer periods of time (Whiteley et al. 2019). While most geotechnical and geophysical landslides studies treat the problem as 2D,

Uhlemann et al. (2017) has shown that geophysical data can be used to image 4D spatio-temporal soil moisture dynamics of landslides prior and post failure, and that thresholds derived from such data can be used as predictor for slope instabilities.

Since geophysical data only provide proxies to the parameters controlling slope stability, such as liquid saturation or pore pressures, integrating geophysical monitoring with wireless sensor networks is becoming more frequently applied. Wireless sensor networks employ distributed point sensing to estimate the variability of those parameters and combine it with the latest developments in wireless data transmission to send data to a processing centre, where data are analysed and used, e.g., for early warning (Ramesh and Vasudevan 2012; Ramesh 2014; Watlet et al. 2019).

Similar to the developments in data acquisition, also modelling has progressed. Now we can model subsurface hydrological and landslide dynamics in 3D and at higher resolution than a decade ago, not only assuming fully saturated, but also partially saturated and conditions that can vary in space and time. Hence, real-world failures can be modelled and those tools be used to predict slope instabilities at local and regional scales.

Monitoring and Early Warning Approach

Our aim is to develop a new methodology that takes advantage of those recent developments to provide reliable early warning of landslide hazards to communities at risk. The methodology is outlined in Fig. 1. and combines geophysical and environmental monitoring with hydrological and geomechanical modelling to estimate and predict slopes FoS, which can be used as a threshold for landslide early warning.

The geophysical and environmental monitoring is providing data regarding groundwater level, soil moisture, rainfall and temperature data, but also information on soil characteristics and structure, e.g. clay content. Those data are then used to parameterize hydrological and slope stability models. Parameters like groundwater level can readily be derived from the geophysical and environmental monitoring data and can be included into the slope stability analysis. Hydrological models are used to provide spatial and temporal distributions of parameters such as pore pressures, which will refine the estimation of stresses in the slopes. Weather predictions can be used to define potential recharge volumes, and hence predict groundwater and pore pressure variations, which, when fed into the geomechanical models, allow to provide future predictions of FoS at local and regional scales. Those predictions can then be used as thresholds for early warning and mitigation measures. In contrast to conventional early warning systems, which are

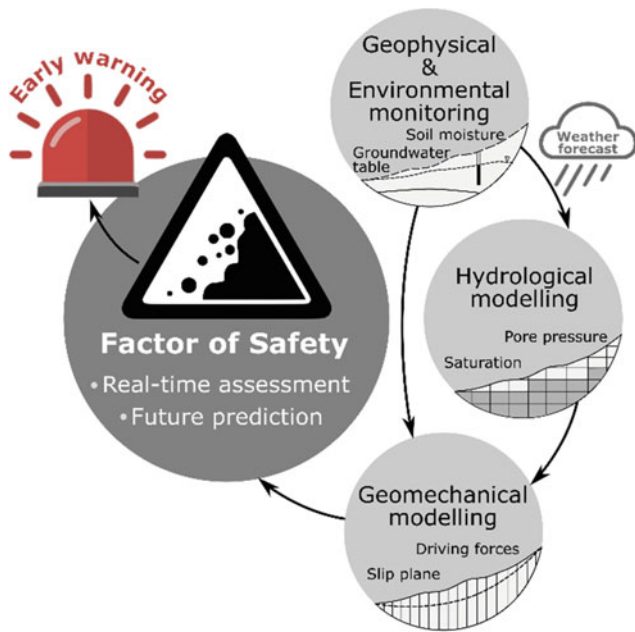


Fig. 1 Methodology for assessment and prediction of slope stability. This workflow integrates the latest developments in geophysical and environmental monitoring with hydrological and geomechanical modelling to provide FoS at local and regional scales that can be used for landslide early warning

mostly reliant on precipitation data only, this approach uses subsurface measurements that are directly linked to the cause of slope instabilities. Hence, we expect these slope stability assessments and predictions to be more reliable.

Study Site

The site to which we apply this methodology is located in the San Francisco Bay Area on the west side of the northwest-trending Berkeley Hills and has a history of slope failures. The landslide investigated here impacts upon a road bridge and has been studied intensively. A ground displacement monitoring system is recording displacements since 2012 and shows movement rates of up to about 10 mm/year, which are correlated with precipitation records (Cohen-Waeber 2018). The landslide can be classified as a very slow moving clay rotational slide (Hungr et al. 2014).

Bedrock geology of the Berkeley Hills is complex and comprises moderately to highly deformed sedimentary, volcanic, and metamorphic rock units. The site itself is located within a mapped landslide deposit (up to 18 m thick) composed of weathered Moraga formation (mainly weathered basalt and andesite flows), which is overlaying Orinda formation, which is composed of partially bedded, non-marine, conglomerate sandstone, and green and red silt- and mudstone. On a regional scale, the Hayward and San Andreas fault are potential sources of seismic activity.

Monitoring Setup

The monitoring setup is shown in Fig. 2. It comprises bi-daily acquisition of Electrical Resistivity Tomography (ERT) data, acquired using a PRIME resistivity monitoring system employing dipole–dipole measurements on 112 electrodes separated by 0.6 m. Hence, subsurface resistivity and changes therein are monitored over a length of 66.6 m and to a depth of approximately 10 m below ground level (bgl). Soil moisture, temperature, and bulk electrical conductivity are measured every 30 min at 20, 40, and 60 m along the ERT monitoring line at 0.1, 0.3, and 0.5 m bgl. Groundwater levels are measured within shallow piezometers (1.83 m bgl) at 20 and 40 m along the ERT line. Precipitation, air temperature and humidity are recorded at a 15 min interval at the toe of the slope. The system is powered using solar energy, and its status is transmitted daily via the Iridium satellite network.

Landslide Structure

Two boreholes in the vicinity of the monitoring site (20–50 m away) indicate weak clay soils of 5.5–7.3 m thickness (paleolandslide deposits) overlying friable sandstones and siltstones of the Orinda formation (Alan Kropp and Associates 2006). This observation is in agreement with the 3D ERT model that was obtained from the site (Fig. 3, recorded at the end of the dry season in November 2019), which shows a low resistive layer (>10 Ωm) above a more resistive

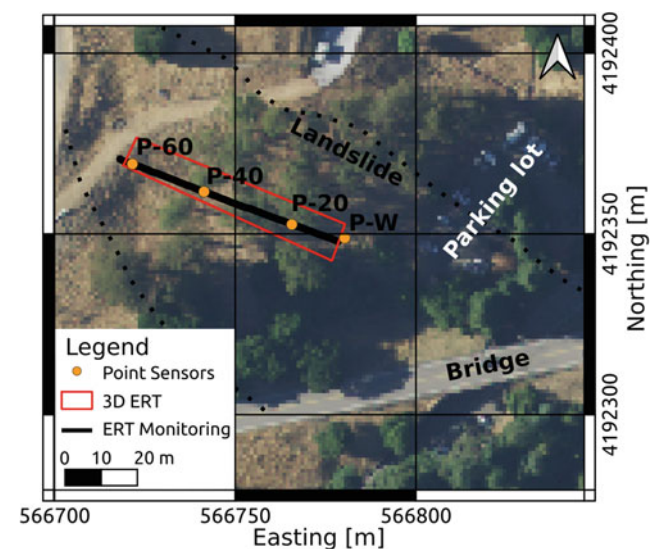


Fig. 2 Map showing 3D ERT data acquisition, ERT monitoring line, and location of point sensors (P-20, P-40, and P-60 soil moisture, temperature and electrical conductivity, P-20 and P-40 include groundwater level monitoring; at P-W precipitation, air temperature and pressure are measured)

layer. On the top of the slope, high resistivities are imaged to deeper depths. This is in agreement with the geological map that indicates a transition from Moraga formation to paleo-landslide deposits in this area. The very low resistive feature in the centre of the volume is interpreted to be fully saturated clay, with the vadose zone and dry clay soils above, and the more resistive Orinda formation below. Hence, the groundwater table is expected to be shallow (1.6–2.0 m bgl) towards the toe of the slope. This is in agreement with previous studies that mapped a periodic spring close to the toe. Note that geophysical inversion, which resulted in the model of Fig. 3, is inherently non-unique. To reduce the model space, we applied a L2 smoothness constraint in space (and time for the monitoring data). As described above, the resulting model is in good agreement with independent geological and hydrological information of the site.

Monitoring Results

The monitoring period has covered rainfall events following an about 6 months long dry period. An initial rainfall event occurred November 25, with significant (>20 mm/d) and prolonged rainfall from December 1st to 13th. This caused soil moisture levels to increase, with every rainfall event showing a rapid increase followed by a gradual decrease in soil moisture, with a downward gradient, indicating downward movement of moisture leading to groundwater recharge. This is also confirmed by the rise in groundwater table from >1.83 m to 1.72 m bgl. After this period, rainfall occurred only occasionally, and with daily accumulations mostly below 20 mm/d. The 2D ERT baseline model (Fig. 4c) shows the same observation as were drawn from

the 3D model, with a highly resistive surface layer, representing dry soil, overlying a layer of low resistivity, spanning from 1.6 m to about 8 m bgl, which is interpreted to be saturated clay. This layer is underlain by a more resistive layer, representative of the sandstone of the Orinda formation.

The rainfall commencing December 1st led to a decrease in resistivity in the majority of the model (Fig. 4d), indicating an increase in soil moisture. The increase in resistivity between about 1.6–3.0 m bgl is assumed to be caused by an exchange of pore waters, with the rainfall providing an input of more resistive pore water.

The rainfall events of late December to January cause only small changes in the resistivity model, with mostly decreasing resistivity values throughout the model. This is indicative of further increases in soil moisture content following a storm event on January 16th. The shallow resistivities (1–2 m bgl) at $x = 20$ and 40 m (blue and orange lines in Fig. 4b, respectively) show this resistivity response to the different rainfall events, with step-like decreases following the storms of December 7th and January 16th, while the period of small rainfall between those caused resistivities to increase slightly at $x = 40$ m, indicating decreasing soil moisture content, as also measured by the point sensor at 0.5 m bgl.

From this data, the location of the groundwater table can be mapped through space and time by extracting the interface between the highly resistive upper layer and the less resistive central layer. This shows that the groundwater table rose by about 0.3 m, particularly in the lower part of the slope, following the rainfall events early December (Fig. 5). The additional rainfall at the end of January 2020 caused an additional rise by about 0.13 m. These observations are in

Fig. 3 Interpreted 3D ERT model of the study site, highlighting the different lithological units, and showing the point sensor locations. Inversion RMS = 4.1%. Blue isovolume showing resistivities <6 Ωm , red isovolume resistivities >30 Ωm

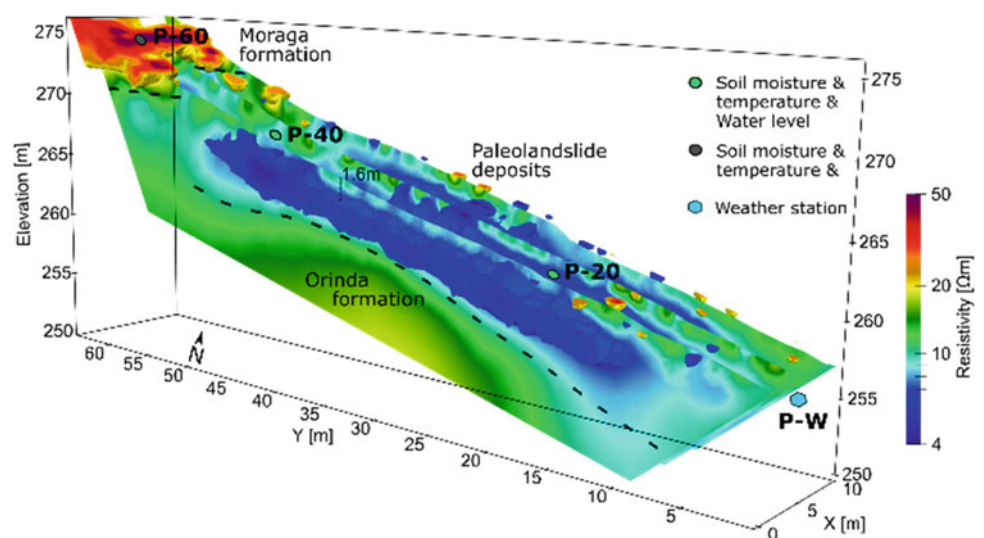


Fig. 4 Geophysical and environmental monitoring data. **a** Precipitation and soil moisture data (at 0.5 m bgl), **b** water level (black line) and average resistivity (shaded area shows the standard deviation) at 1–2 m bgl at two locations, **c** ERT baseline model, **d–e** change in resistivity compared to baseline model

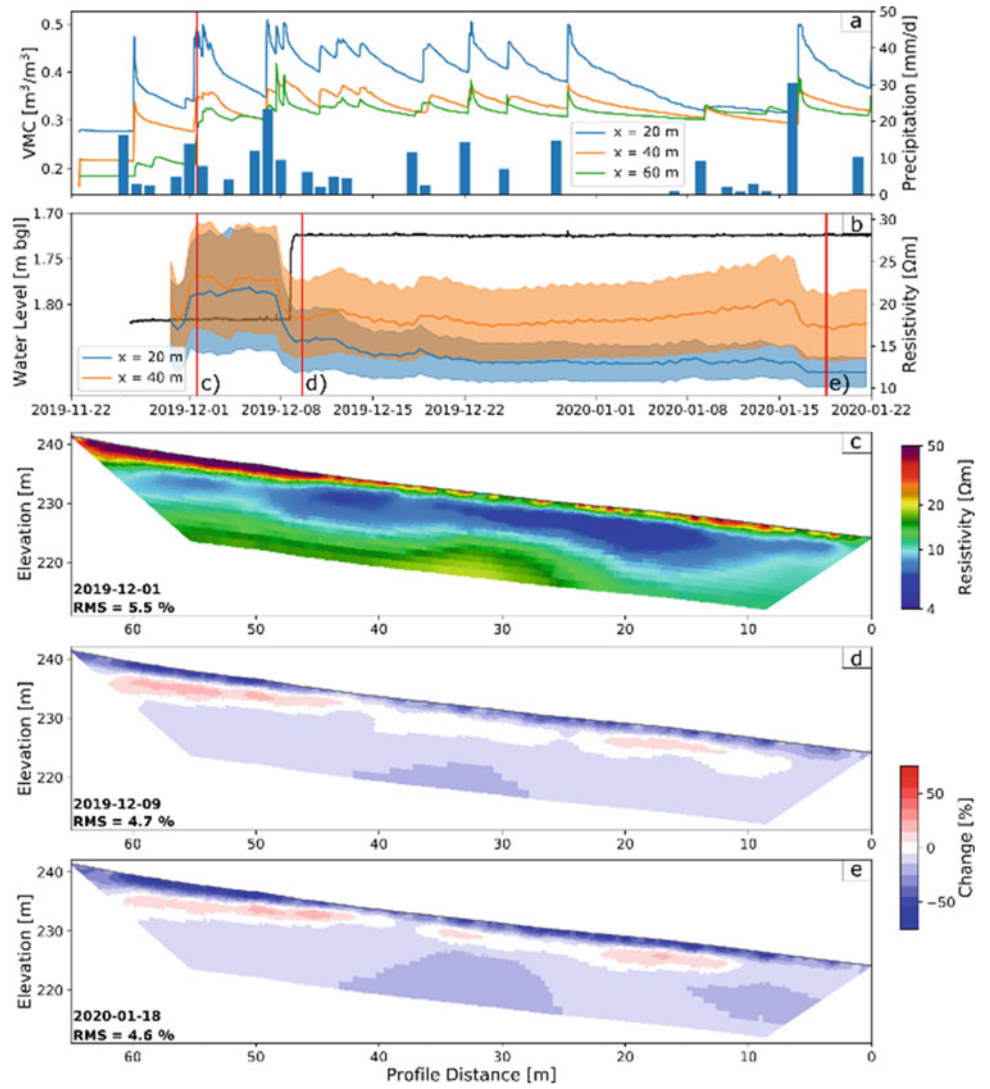
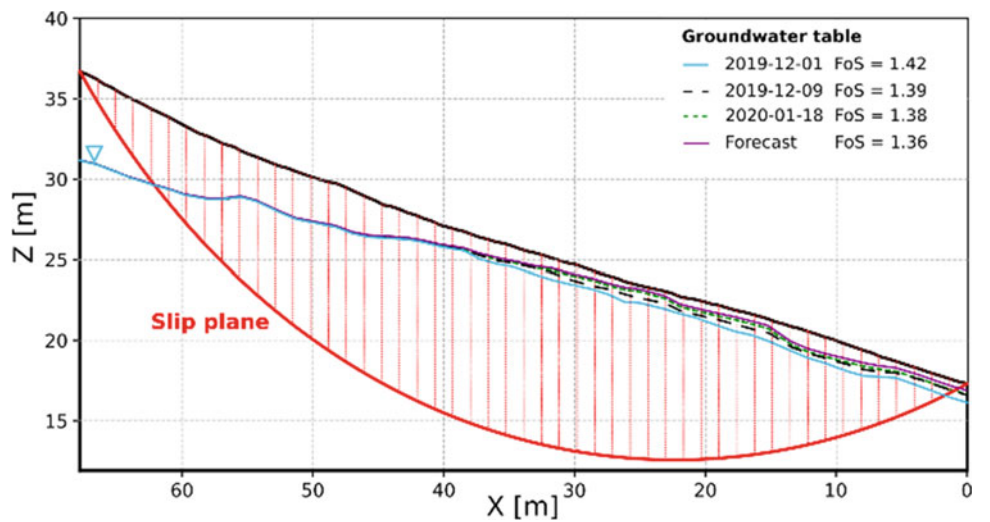


Fig. 5 Simplified slope stability analysis, accounting for the groundwater table variations as mapped from the ERT data. The FoS for a dry slope (i.e. groundwater table below the slip plane) is 2.21, the FoS for the different groundwater conditions is provided in the legend



broad agreement with the groundwater table and soil moisture measurements obtained from site.

Using a groundwater flow model (PFLOTRAN, Hammond et al. 2014), we estimated that a rainfall period similar to the one observed early December would cause the groundwater table to rise on average by 0.21 m from the January 2020 conditions.

Slope Stability Analysis and Prediction

To introduce our approach, we simplify the slope stability problem. Given that the paleolandslide deposits were mapped with a thickness of up to 18 m and that the top of the Orinda formation showed a similar friable characteristic to the overlying soil in soil borings close by, we assume that the slope consists of one soil type only and that the failure type is rotational.

The FoS of the slope is determined for the different groundwater conditions using the General Limit Equilibrium method (Fredlund and Krahn 1977) implemented in the python code `pyBIMstab` (Montoya-Araque and Suarez-Burgoa 2018), and satisfies both force and moment equilibrium. Previous studies found the soil to have an effective cohesion of 7.75 kPa, a unit weight of 18.85 kN/m³, and a friction angle of 24° (Alan Kropp and Associates 2006). Analysing more than 5000 possible slip surfaces, Fig. 5 shows the slip surface with the smallest FoS and thus the most likely slip plane. With a maximum depth of about 12 m, this result is in agreement with previous site investigations.

For dry conditions, i.e. the groundwater table is below the proposed slip plane, the FoS is 2.21 and the slope stable. From the piezometer and ERT data we can derive the location of the groundwater table at different times. Including the conditions of December 1st in the analysis results in a FoS of 1.42 (Fig. 5). The prolonged and intense rainfall between December 1st and 13th caused a rise in groundwater table that reduces the FoS to 1.39. The groundwater conditions following the storm on January 16th caused a further reduction of the FoS to 1.38. Continuing from those conditions and simulating another storm with similar precipitation to the one observed early December would cause another rise in groundwater table and hence reduce the FoS to 1.36.

Although simplified and of limited monitoring length, these results show the benefit of including estimated and modelled hydrological subsurface conditions into the slope stability analysis. It allows to provide a well-informed estimate of current conditions. In addition, by modelling the impact of future precipitation events on the subsurface conditions, slope stability in response to these events can be predicted. While we showed the feasibility of this approach,

we could not validate an early warning threshold, as the slope remained stable during the monitoring period.

This approach is limited by the accuracy and availability of the geophysical and environmental data, as well as the model validity for both hydrological and geomechanical simulations. Wrong parameterization of the model may provide erroneous, and hence misleading, FoS estimates. Nevertheless, we anticipate that incorporating subsurface information into the early warning methodology will improve our predictions.

Future work will increase the complexity of both hydrological and slope stability models, by including subsurface layers with different physical properties and extending the domain from 2D to 3D. Applying this to a regional scale will increase computational time significantly, and hence new approaches have to be developed to provide estimates and predictions of slope stability in near real-time.

Conclusions

Landslide early warning is still mostly reliant on regionally defined rainfall thresholds. Here, we introduce a methodology that combines the latest developments in geophysical and environmental monitoring, with hydrological and geomechanical modelling to provide robust estimates of slope stability and predict its evolution for future precipitation events by including measured and estimated subsurface conditions.

We introduce this approach using data from a study site in Northern California with a history of slope instabilities. From Electrical Resistivity Tomography (ERT) data and a distributed sensor network, subsurface conditions and variations in groundwater table are estimated and included in the slope stability analysis. Using a hydrological model, the impact of a potential future storm event on the groundwater conditions are derived and included in the geomechanical model to predict its impact on the slope stability. During all conditions, the FoS of the slope is greater than 1, but the changes in subsurface conditions following winter storms show a reduction of the FoS, and hence an increase in potential failure likelihood.

While this approach has been applied to a local hill slope, it could easily be up-scaled and applied to a regional scale using emerging remote sensing products for subsurface characterization (e.g. airborne electromagnetics to map soil–bedrock interface) and monitoring (e.g. radar-based shallow soil moisture measurements), and wireless sensor networks to provide distributed soil moisture data on regional grids. Using 5G networks, this data could be used real-time to update current slope stability models. By including weather forecasts, slope stability could be forecasted and early warning given to communities at risk, well in advance of

potentially hazardous conditions. This will ultimately reduce landslide risk and will aid in protecting vulnerable communities.

Acknowledgements This work has been funded by an Early Career Development Grant awarded to Sebastian Uhlemann by the Earth and Environmental Sciences Area of Berkeley Lab. The contribution of Jonathan Chambers and Philip Meldrum is published with the permission of the Executive Director of the British Geological Survey (NERC).

References

- Alan Kropp and Associates I (2006) Initial landslide characterization study East Canyon—Buildings 85 and 85A
- Bogaard TA, Greco R (2016) Landslide hydrology: from hydrology to pore pressure. *Wiley Interdiscip Rev Water* 3:439–459
- Bordoni M, Meisina C, Valentino R et al (2015) Hydrological factors affecting rainfall-induced shallow landslides: from the field monitoring to a simplified slope stability analysis. *Eng Geol* 193:19–37
- Cohen-Waeber J (2018) Spatiotemporal patterns of seasonality in landslide deformation from InSAR and GPS. PhD thesis, UC Berkeley
- Fredlund DG, Krahn J (1977) Comparison of slope stability methods of analysis. *Can Geotech J* 14:429–439
- Godt JW (1999) Maps showing locations of damaging landslides caused by El Nino rainstorms, winter season 1997–98. San Francisco Bay Region, California
- Hammond GE, Lichtner PC, Mills RT (2014) Evaluating the performance of parallel subsurface simulators: an illustrative example with PFLOTRAN. *Water Resour Res* 50:208–228
- Hinnell AC, Ferré TPA, Vrugt JA et al (2010) Improved extraction of hydrologic information from geophysical data through coupled hydrogeophysical inversion. *Water Resour Res* 46:1–14
- Hungr O, Leroueil S, Picarelli L (2014) The Varnes classification of landslide types, an update. *Landslides* 11:167–194
- Huntley D, Bobrowsky P, Hendry M et al (2019) Application of multi-dimensional electrical resistivity tomography datasets to investigate a very slow-moving landslide near Ashcroft, British Columbia, Canada. *Landslides* 16:1033–1042
- Irving J, Singha K (2010) Stochastic inversion of tracer test and electrical geophysical data to estimate hydraulic conductivities. *Water Resour Res* 46:1–16
- Johnson TC, Hammond GE, Chen X (2017) PFLOTRAN-E4D: a parallel open source PFLOTRAN module for simulating time-lapse electrical resistivity data. *Comput Geosci* 99:72–80
- Marra F (2019) Rainfall thresholds for landslide occurrence: systematic underestimation using coarse temporal resolution data. *Nat Hazards* 95:883–890
- Montoya-Araque EA, Suarez-Burgoa LO (2018) pyBIMstab: application software for 2D slope stability analysis of block-in-matrix and homogeneous materials. *SoftwareX* 7:383–387
- Ramesh MV (2014) Design, development, and deployment of a wireless sensor network for detection of landslides. *Ad Hoc Netw* 13:2–18
- Ramesh MV, Vasudevan N (2012) The deployment of deep-earth sensor probes for landslide detection. *Landslides* 9:457–474
- Singha K, Day-Lewis FD, Johnson T, Slater LD (2015) Advances in interpretation of subsurface processes with time-lapse electrical imaging. *Hydrol Process* 29:1549–1576
- Springman SM, Kienzler P, Friedel S et al (2013) A long-term field study for the investigation of rainfall-induced landslides. *Geotechnique* 63:1177–1193
- Uhlemann S, Chambers J, Wilkinson P et al (2017) Four-dimensional imaging of moisture dynamics during landslide reactivation. *J Geophys Res Earth Surf* 122:1–21
- Watlet A, Thirugnanam H, Singh B et al (2019) Deployment of an electrical resistivity monitoring system to monitor a rainfall-induced landslide (Munnar, India). In: AGU fall meeting 2019, 9–13 December, San Francisco, USA
- Whiteley JS, Chambers JE, Uhlemann S et al (2019) Geophysical monitoring of moisture-induced landslides: a review. *Rev Geophys* 57:106–145